

### ${}^9\text{Be}(t,p){}^{11}\text{Be}$ and the structure of ${}^{11}\text{Be}$

G.-B. Liu\* and H. T. Fortune

*Physics Department, University of Pennsylvania, Philadelphia, Pennsylvania 19104*

(Received 30 June 1989; revised manuscript received 25 April 1990)

The  ${}^9\text{Be}(t,p){}^{11}\text{Be}$  reaction has been used to populate the low-lying states with a 15-MeV triton beam. Differential cross sections were measured for nine low-lying states and distorted-wave Born-approximation calculations were used to analyze the data. Contributions from  $p$ -shell,  ${}^{10}\text{Be}\otimes(sd)^1$ , and  ${}^9\text{Be}(g.s.)\otimes(sd)^2$  configurations were investigated. The dominant structure is suggested for nearly all states investigated in the present work.

#### I. INTRODUCTION

The  ${}^{11}\text{Be}$  nucleus has been the object of a series of studies,<sup>1-3</sup> and its low-lying levels are compiled in a recent paper.<sup>4</sup> Pullen *et al.*<sup>5</sup> used the  ${}^9\text{Be}(t,p){}^{11}\text{Be}$  reaction at lower beam energies and measured the natural widths of three states at 1.78, 2.70, and 3.41 MeV. Ajzenberg-Selove *et al.*<sup>6</sup> measured the angular distributions for eight states in the same reaction. However, they did not present a detailed analysis based on distorted-wave Born-approximation (DWBA) calculations. The  ${}^{10}\text{Be}(d,p){}^{11}\text{Be}$  reaction has also been used to populate the states of  ${}^{11}\text{Be}$  (Refs. 7 and 8). Transfer angular momenta for ground state (g.s.), 0.32-, and 1.78-MeV states were found to be 0, 1, and 2, respectively.

The  $\frac{1}{2}^+$  ground state and the (probable)  $\frac{5}{2}^+$  level at 1.78 MeV are undoubtedly described as an  $sd$ -shell neutron coupled to  ${}^{10}\text{Be}(g.s.)$ . Low-lying negative-parity states could be purely  $p$  shell in character, i.e.,  ${}^{16}\text{O}\otimes(1p)^{-5}$ . However, more states are known experimentally than are calculated in a  $p$ -shell basis as, e.g., by Cohen and Kurath.<sup>9,10</sup> These additional negative-parity levels are probably of the form  ${}^9\text{Be}\otimes(sd)^2$ . All three types of states can be populated by  ${}^9\text{Be}(t,p){}^{11}\text{Be}$ . For the Cohen-Kurath (CK) states,<sup>9</sup> the two transferred neutrons will populate the  $1p$  shell. For the positive-parity levels, one of the transferred neutrons will enter the  $1p$  shell and the other an  $sd$  orbital. The third type of state will have negative parity and will be populated in  $(t,p)$  by having both neutrons transferred into the  $sd$  shell. Figure 1

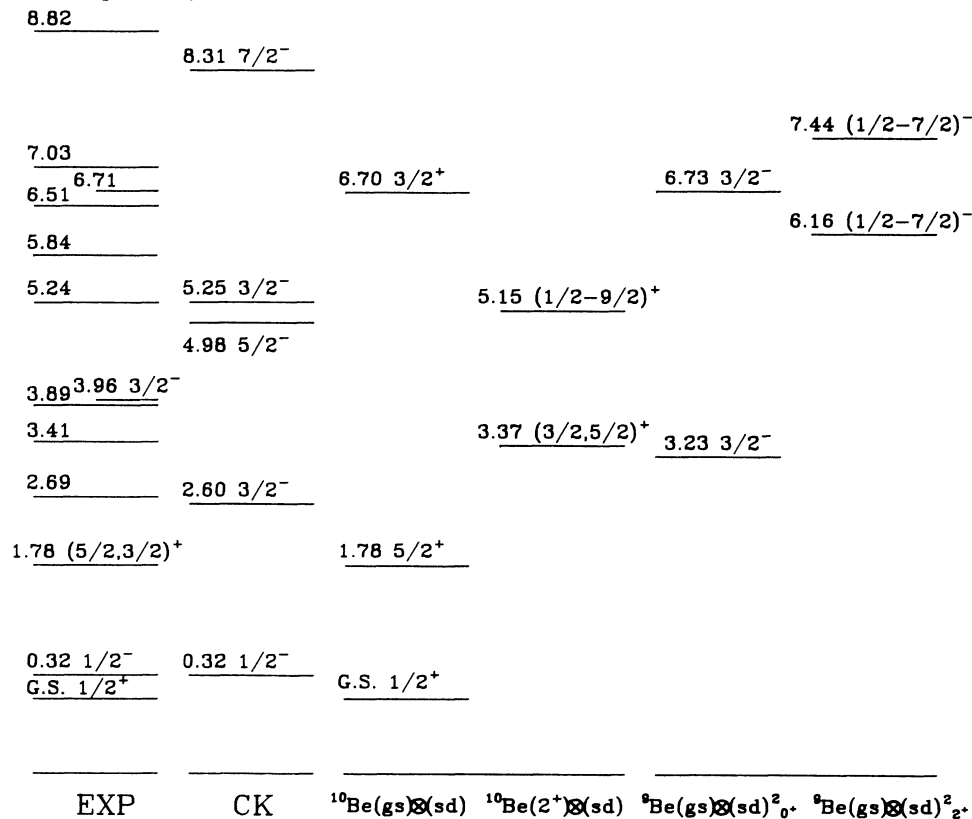


FIG. 1. Experimental and theoretical energy levels of  ${}^{11}\text{Be}$ .

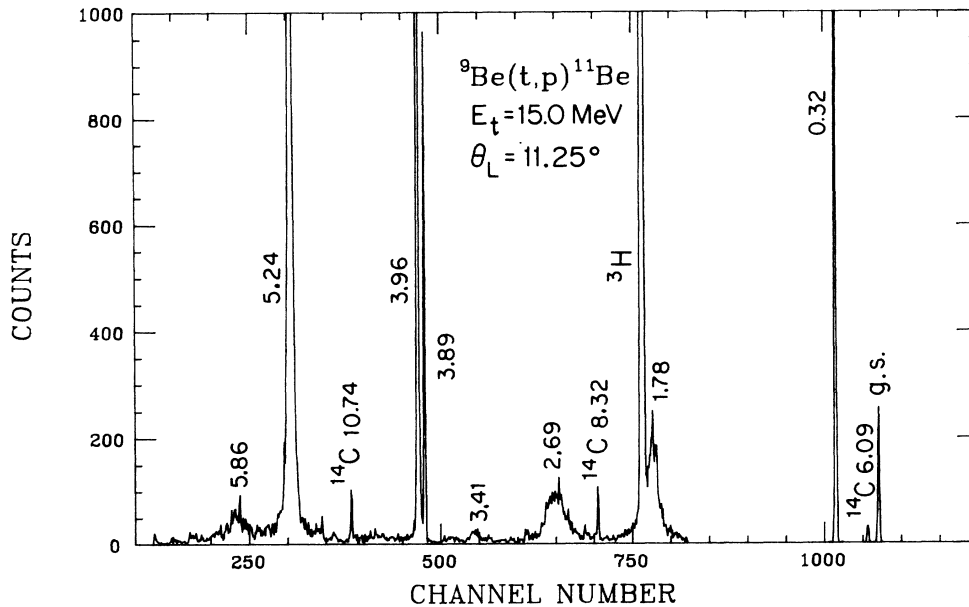


FIG. 2. Spectrum of the reaction  ${}^9\text{Be}(t,p){}^{11}\text{Be}$ . States in  ${}^{11}\text{Be}$  are labeled by their excitation energies. Peaks from impurities in the target are labeled by final nucleus and their excitation energy.

displays a level diagram of the possible states from these three different types of configuration. We will come back to this point later. The main purpose of the present experiment is to determine the dominant structure of the low-lying states observed in the reaction  ${}^9\text{Be}(t,p){}^{11}\text{Be}$ . Of course, each type of state continues to higher excitation energies, above those our experiment could reach.

## II. EXPERIMENTAL PROCEDURE

The experiment was performed with a 15.0-MeV triton beam from the University of Pennsylvania tandem accelerator. The target was a  $65\text{-}\mu\text{g}/\text{cm}^2$   ${}^9\text{Be}$  foil. Outgoing protons were momentum analyzed in a multiangle spectrograph and detected in nuclear emulsion plates. Data were recorded in  $7.5^\circ$  steps beginning at  $3.75^\circ$ . A typical spectrum of protons is displayed in Fig. 2. The resolution is about 28 keV FWHM. Five narrow states and four broad ones of  ${}^{11}\text{Be}$  are identified. A number of

impurity peaks are also apparent and are labeled by final nucleus and excitation energy. Below 6-MeV excitation energy, our data allow us to set an upper limit of  $10\ \mu\text{b}/\text{sr}$  (1% of the 0.32-MeV state cross section) for any possible missing narrow state.

## III. RESULTS AND ANALYSIS

The evaluated excitation energies and level widths from this experiment are compared with previous data in Table I. The width of the 5.86-MeV state is found to be  $139\pm 17$  keV and is much smaller than the previous value ( $\approx 300$  keV) (Ref. 4). Except for this large difference, the other values are all consistent with the previous data within the experimental errors. In the last column of the table, we list the integrated cross section  $\sigma_{\text{tot}}$  of data between  $0^\circ$  and  $60^\circ$  (c.m.) for each state. In Fig. 3, differential cross sections for the nine lowest states of  ${}^{11}\text{Be}$  are shown. Error bars in the figures are statistical

TABLE I. Results of the reaction  ${}^9\text{Be}(t,p){}^{11}\text{Be}$  and previous information

$E_x$ (MeV)	Previous <sup>a</sup>		Present		$\sigma_{\text{tot}}^{\text{b}}$ (mb)
	Width (keV)	$E_x$ (MeV $\pm$ keV)	Width (keV)		
0.0		$-0.004\pm 3$			$0.491\pm 0.025$
0.320		$0.320\pm 2$			$2.214\pm 0.111$
1.778	$100\pm 20$	$1.748\pm 4$	$104\pm 21$		$1.746\pm 0.087$
2.69	$200\pm 20$	$2.642\pm 9$	$228\pm 21$		$1.144\pm 0.057$
3.41	$125\pm 20$	$3.398\pm 6$	$104\pm 17$		$0.404\pm 0.020$
3.89	$< 10$	$3.888\pm 1$			$1.081\pm 0.054$
3.96	$15\pm 5$	$3.955\pm 1$			$2.376\pm 0.119$
5.24	$45\pm 10$	$5.255\pm 3$			$3.386\pm 0.169$
(5.86)	$\sim 300$	$5.849\pm 10$	$139\pm 17$		$0.531\pm 0.027$

<sup>a</sup>See Ref. 4.

<sup>b</sup> $0^\circ$ – $60^\circ$  (CM).

TABLE II. Optical-model parameters used in analysis of  ${}^9\text{Be}(t,p){}^{11}\text{Be}$  (Strengths in MeV, lengths in fm).

Channel	$V$	$r_0$	$a_0$	$W$	$4W'$	$r'_0$	$a'_0$	$V_{s.o}$	$r_c$
$t$	130.0	1.29	0.58	18.90		1.37	0.96		1.29
$p$	60.00	1.13	0.57		34.20	1.13	0.57	5.50	1.13
Bound state		1.26	0.60					$\lambda=25.0$	1.20

and the absolute scale has an uncertainty of about 15%. Angular resolution is a fraction of  $1^\circ$ . The curves in the figure result from local, zero-range, microscopic DWBA calculations, using code DWUCK4.<sup>11</sup> The optical parameters used in the calculations are listed in Table II.<sup>12</sup>

As we mentioned before, there are three types of states

populated in the  ${}^9\text{Be}(t,p){}^{11}\text{Be}$  reaction. In Fig. 1, these three types of states are presented and compared with the experimental levels. The states at 0.32-MeV  $\frac{1}{2}^-$  and 2.60-MeV  $\frac{3}{2}^-$  in the second column of the figure probably correspond to  $p$ -shell states (CK). Here we line up the 0.32-MeV state (CK) with the experimental 0.32-MeV

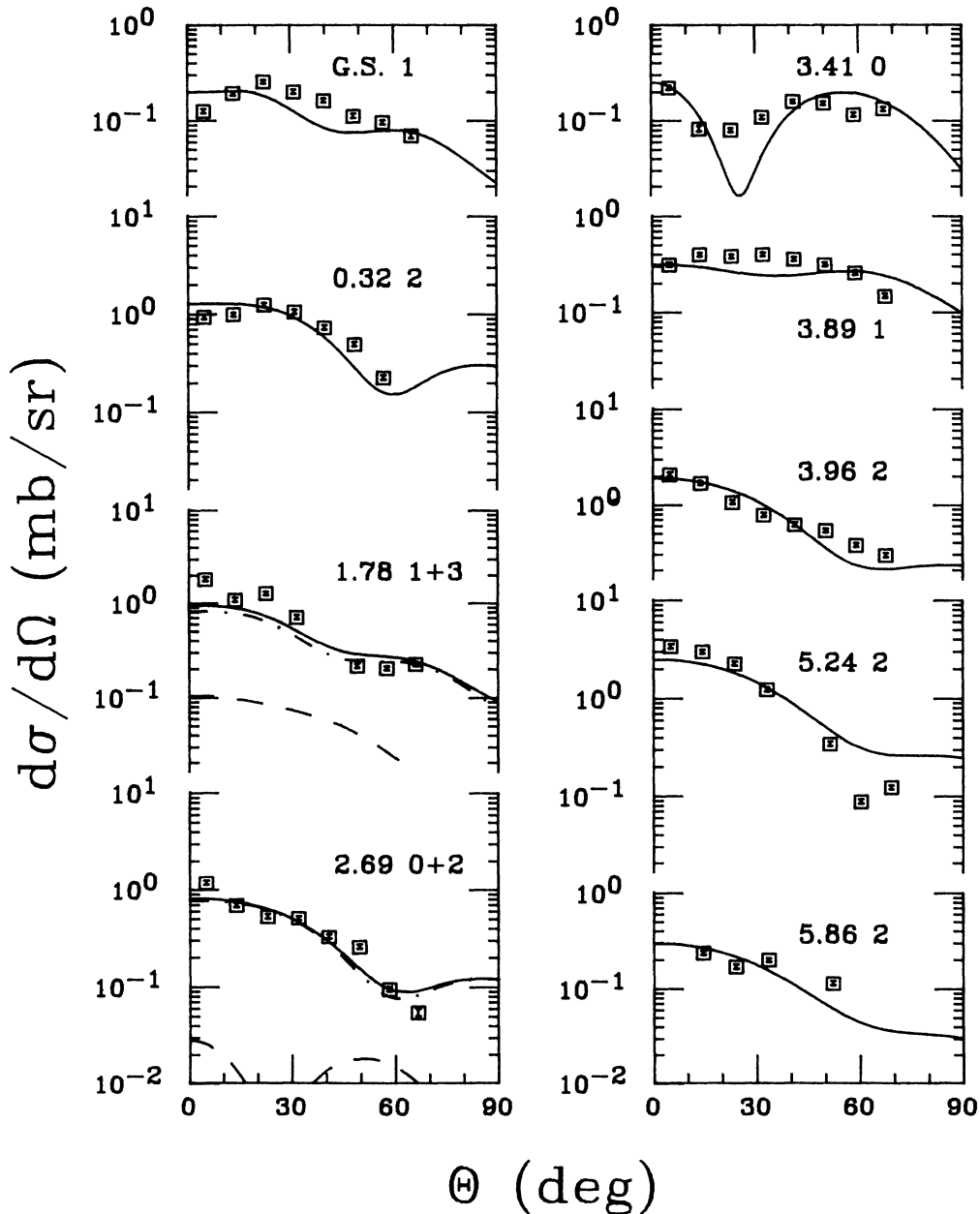


FIG. 3. Angular distributions of states populated in the reaction  ${}^9\text{Be}(t,p){}^{11}\text{Be}$ . Curves are the results of DWBA calculation with arbitrary normalizations.

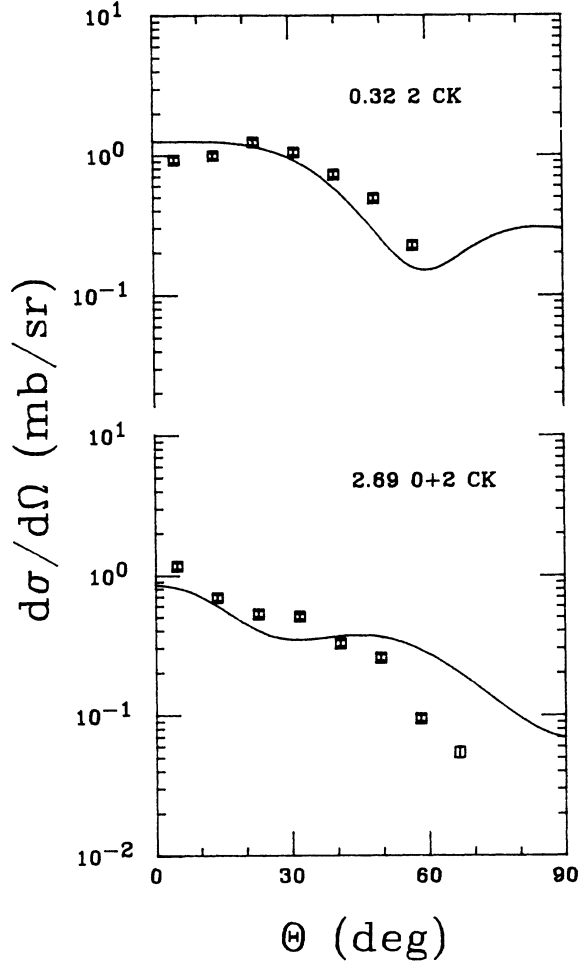


FIG. 4. Angular distributions for two predominantly  $p$ -shell states. Curves are normalized as given in Table III.

state. In Fig. 4, we compare the data of these two states with DWBA calculations based on CK wave function. The transferred angular momentum for the 0.32-MeV state is pure  $L=2$  and that for the 2.69-MeV state is mainly  $L=2$  with a small amount of  $L=0$  transfer (see Fig. 3).

The second type of state is assumed to be an  $sd$ -shell neutron couple to the g.s.  $0^+$  or 3.368-MeV  $2^+$  level of  $^{10}\text{Be}$ . These states are shown in the third and fourth columns of Fig. 1, respectively. We assume the  $\frac{1}{2}^+$  ground state of  $^{11}\text{Be}$  and the 1.78-MeV  $\frac{5}{2}^+$  state can be expressed as  $^{10}\text{Be}(\text{g.s.}) \otimes (s\frac{1}{2})$  and  $^{10}\text{Be}(\text{g.s.}) \otimes (1d\frac{5}{2})$ , respectively. The 3.89-MeV state of  $^{11}\text{Be}$  could be of a similar nature except coupled to the 3.368-MeV  $2^+$  state of  $^{10}\text{Be}$  instead of its ground state. This configuration could be expressed as  $^{10}\text{Be}(2^+) \otimes (s\frac{1}{2})$ . Here the amplitude needed for DWBA calculation is not 1.0. We need the amplitude for two-neutron transfer from  $^9\text{Be}(\text{g.s.})$  to states of the form  $^{10}\text{Be}(\text{g.s.}) \otimes (sd)$  or  $^{10}\text{Be}(2^+) \otimes (sd)$ . For the  $^{11}\text{Be}(1/2^+)$  state, we write

$$^9\text{Be}(\text{g.s.}) \otimes (1p\frac{3}{2}, 2s\frac{1}{2})_{L=1} = U([^9\text{Be}(\text{g.s.}) \otimes (1p\frac{3}{2})]_{0^+} \otimes (2s\frac{1}{2}))$$

and use a spectroscopic amplitude  $\sqrt{S}=1.45$  for  $^9\text{Be}(\text{g.s.}) \rightarrow ^{10}\text{Be}(\text{g.s.})$  (Ref. 13), and unity for  $^{10}\text{Be}(\text{g.s.}) \rightarrow ^{11}\text{Be}(\frac{1}{2}^+)$ . The  $6J$  coefficient needed is that for

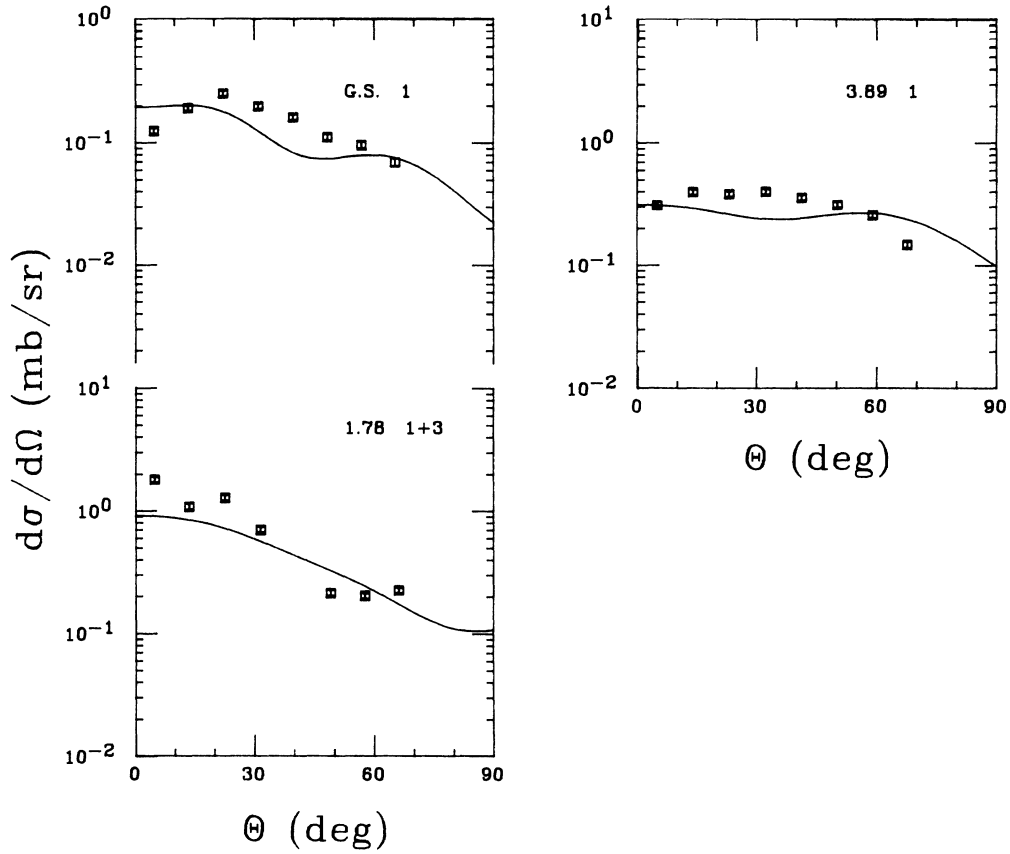
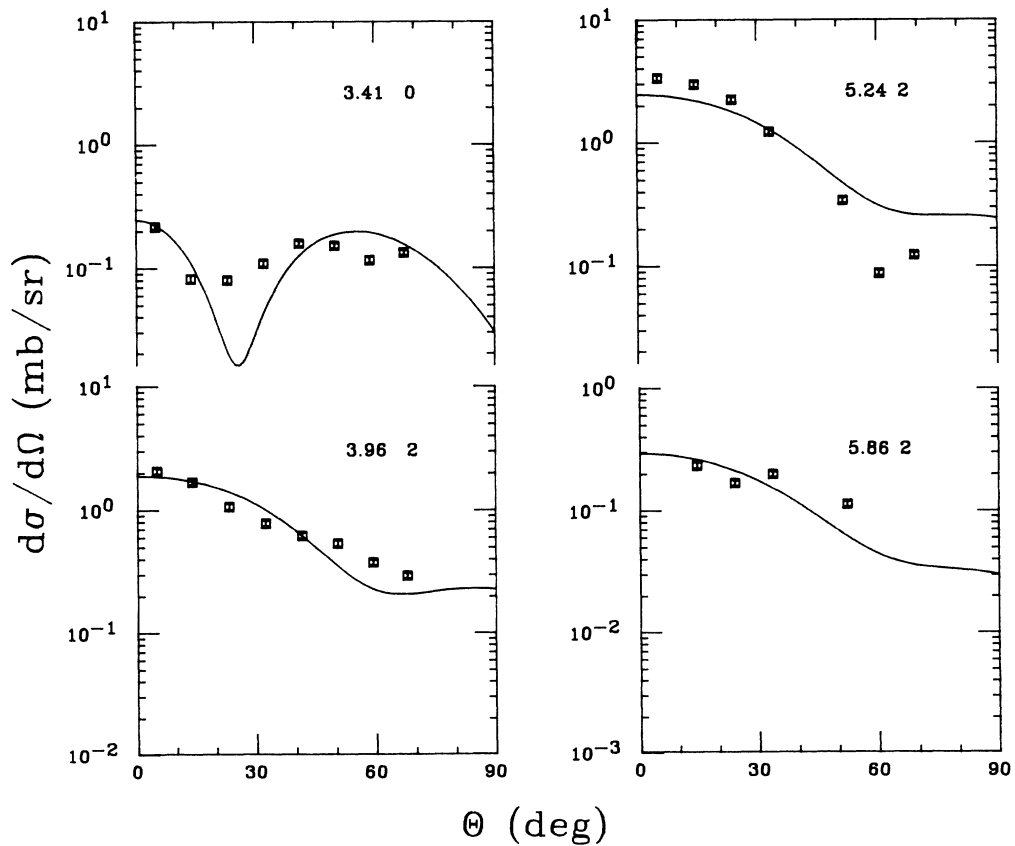
$$[(j_1 j_3)_{j_{13}} j_2]_{J_f} \rightarrow [j_1 (j_3 j_2)_{j_{23}}]_{J_f},$$

where  $j_1, j_2, j_3, j_{13}, j_{23}$ , and  $J_f$  are angular momenta of  $\frac{3}{2}$  for  $^9\text{Be}(\text{g.s.})$ ,  $\frac{1}{2}$  of  $v(2s\frac{1}{2})$ ,  $\frac{3}{2}$  of  $v(1p\frac{3}{2})$ , 0 of  $^{10}\text{Be}(\text{g.s.})$ , 1 of  $v(1p\frac{3}{2}) \otimes v(2s\frac{1}{2})$  coupling, and  $\frac{1}{2}$  of final state  $^{11}\text{Be}(\text{g.s.})$ , respectively. For the other two couplings mentioned previously, corresponding evaluations are needed in order to obtain amplitudes to be used in DWBA calculations. In Fig. 5, differential cross sections for these states and DWBA calculations with the mentioned configuration and amplitudes are presented.

The last two columns in Fig. 1 list possible states that should be reached through two ( $sd$ )-shell neutron transfer; their configuration could be written as  $^9\text{Be}(\text{g.s.}) \otimes (sd)_{0^+}^2$  (fifth column) and  $^9\text{Be}(\text{g.s.}) \otimes (sd)_{2^+}^2$  (sixth column). In order to perform DWBA calculation, we need to obtain an amplitude for this kind of

TABLE III. Configuration mixture for  $^{11}\text{Be}$  states.

$E_x$ (MeV)	$J^\pi$ (prev)	$L$	Configuration	$J^\pi$ (present)	$N$
0.0	$\frac{1}{2}^+$	1	$^{10}\text{Be}(\text{g.s.}) \otimes (s\frac{1}{2})$	$\frac{1}{2}^+$	167.9
0.32	$\frac{1}{2}^-$	2	CK	$\frac{1}{2}^-$	617.7
1.78	$(\frac{5}{2}, \frac{3}{2})^+$	1+3	$^{10}\text{Be}(\text{g.s.}) \otimes (d\frac{5}{2})$	$\frac{5}{2}^+$	50.53
2.69		0+2	CK	$\frac{3}{2}^-$	255.8
3.41		0	$^9\text{Be}(\text{g.s.}) \otimes (sd)_{0^+}^2$	$\frac{3}{2}^-$	85
3.89	$\geq \frac{7}{2}$	1	$^{10}\text{Be}(2^+) \otimes (s\frac{1}{2})$	$\frac{3}{2}^+$	274.2
3.96	$\frac{3}{2}^-$	2	$^9\text{Be}(\text{g.s.}) \otimes (sd)_{2^+}^2$	$\frac{3}{2}^-$	266.2
5.24		2	$^9\text{Be}(\text{g.s.}) \otimes (sd)_{2^+}^2$	$\frac{5}{2}^-$	315.5
5.86		1	$^{10}\text{Be}(2^+) \otimes (d\frac{5}{2})$	$\frac{1}{2}^+$	11448
5.86		2	$^9\text{Be}(\text{g.s.}) \otimes (sd)_{2^+}^2$	$\frac{1}{2}^-$	143.3

FIG. 5. As Fig. 4, but for probable  ${}^{10}\text{Be} \otimes sd$  state.FIG. 6. As Fig. 4, but for probable  ${}^9\text{Be} \otimes (sd)^2$  states.

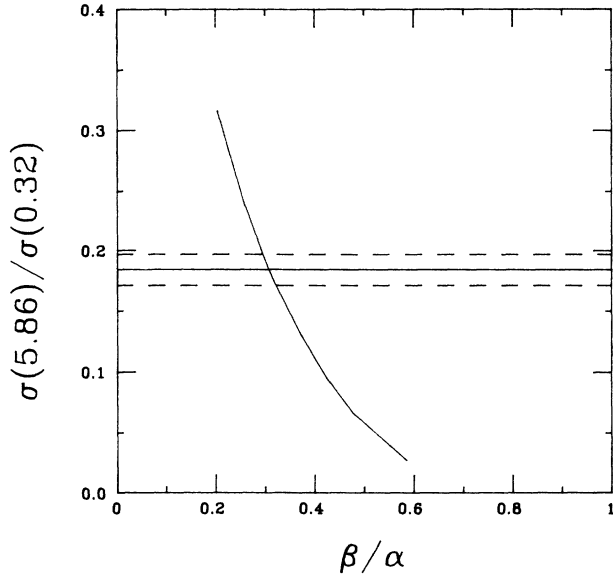


FIG. 7. Calculated cross-section ratio  $\sigma(5.86)/\sigma(0.32)$  vs  $\beta/\alpha$ ; see text.

configuration.

We make the simple assumptions that  $(sd)^2 0^+$  and  $2^+$  states are weakly coupled to  ${}^9\text{Be}(\text{g.s.})$  and that the  $(sd)^2$  states can be approximated as eigenfunctions of  $2 \times 2$  Hamiltonians, ignoring the  $1d_{3/2}$  orbital. For  $L=0$  transfer, we have

$$H_{0^+} = \begin{Bmatrix} 2E_b(s_{\frac{1}{2}}) + V(\frac{1}{2}, \frac{1}{2}; \frac{1}{2}, \frac{1}{2}) & V(\frac{1}{2}, \frac{1}{2}; \frac{5}{2}, \frac{5}{2}) \\ V(\frac{1}{2}, \frac{1}{2}; \frac{5}{2}, \frac{5}{2}) & 2E_b(d_{\frac{5}{2}}) + V(\frac{5}{2}, \frac{5}{2}; \frac{5}{2}, \frac{5}{2}) \end{Bmatrix}$$

and for  $L=2$  transfer, we have a similar matrix as

$$H_{2^+} = \begin{Bmatrix} E_b(s_{\frac{1}{2}}) + E_b(d_{\frac{5}{2}}) + V(\frac{5}{2}, \frac{1}{2}; \frac{5}{2}, \frac{1}{2}) & V(\frac{5}{2}, \frac{1}{2}; \frac{5}{2}, \frac{5}{2}) \\ V(\frac{5}{2}, \frac{1}{2}; \frac{5}{2}, \frac{5}{2}) & 2E_b(d_{\frac{5}{2}}) + V(\frac{5}{2}, \frac{5}{2}; \frac{5}{2}, \frac{5}{2}) \end{Bmatrix},$$

where  $E_b(s_{\frac{1}{2}})$  and  $E_b(d_{\frac{5}{2}})$  are binding energies of  $(2s_{\frac{1}{2}})$  and  $(1d_{\frac{5}{2}})$  single neutrons, respectively (which we took to be  $-0.549$  and  $0.373$  MeV);  $V(jj, jj)$ s are matrix elements from Table VII of Ref. 14. After diagonalizing, we get two eigenvalues and two sets of wave functions for each case. The eigenvalues are shown in last two columns of Fig. 1. The wave functions are used in DWBA calculations. In Fig. 6, we compare the data for the 3.41-, 3.96-, 5.24-, and 5.86-MeV states of  ${}^{11}\text{Be}$  with DWBA calculations with the mentioned configurations in Fig. 1.

In Table III, we summarize the configurations used in the DWBA calculations for each state. The suggested  $J^\pi$  assignments for these states are based on comparison between experimental data and DWBA calculations, and they are also listed in the table. For the two-nucleon transfer reaction, we have

$$\sigma_{\text{exp}} = N \frac{2J_f + 1}{2J_i + 1} \sum_L \frac{\sigma_{dw}}{2L + 1},$$

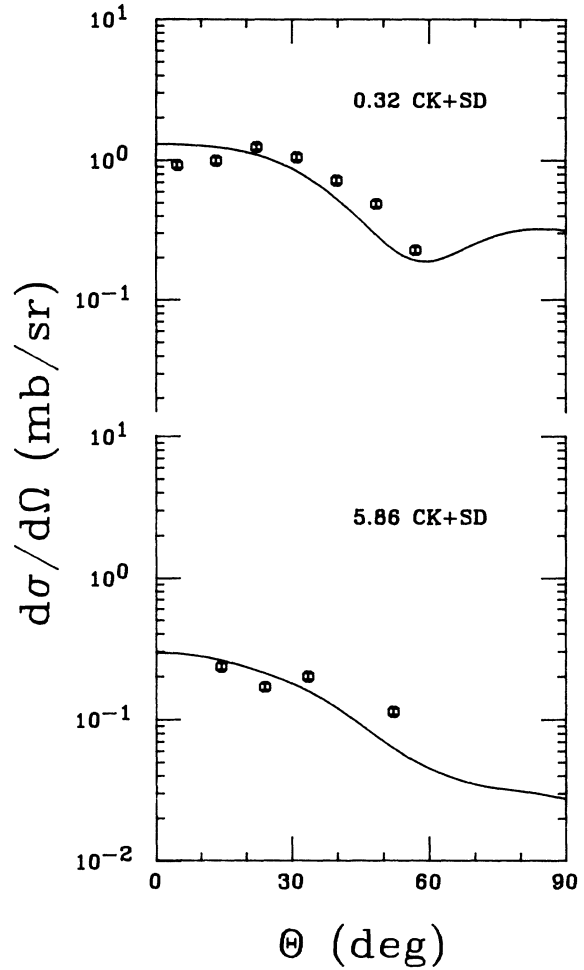


FIG. 8. Experimental cross sections and mixed DWBA calculations; see text.

where  $J_f$ ,  $J_i$  and  $L$  are final, initial, and transferred angular momenta. The evaluated normalization factor  $N$  for each state is listed in the last column of Table III. In other  $(t, p)$  reactions in this mass region (see, e.g., Ref. 12), values of  $N$  range from 200–400 when realistic wave functions are employed. There is a possible configuration mixture between the CK- and  $(sd)^2$  wave function for the same transferred  $L$ . In Table III, e.g., the overall normalization factor  $N = 618$  of 0.32-MeV state is too large, implying possibly some contribution from  $(sd)$ -shell transfer, which we did not take into account. In contrast, an  $N$  of 143 for the 5.86-MeV state is too small. Similarly, some contribution from the CK wave function needs to be considered. To estimate possible mixing, we assume

$$|0.32\rangle = \alpha|\text{CK}\rangle + \beta|(sd)^2\rangle,$$

$$|5.86\rangle = -\beta|\text{CK}\rangle + \alpha|(sd)^2\rangle,$$

and

$$\alpha^2 + \beta^2 = 1,$$

where  $\alpha$  and  $\beta$  are mixture amplitudes for 0.32- and 5.86-MeV states, and  $|x\rangle$ 's are corresponding wave functions. Varying  $\beta/\alpha$ , and calculating cross sections using DWBA with the mentioned configuration mixtures, we get ratios of  $\sigma(5.86)/\sigma(0.32)$ . In Fig. 7,  $\sigma(5.86)/\sigma(0.32)$  is plotted versus  $\beta/\alpha$ , and the experimental ratio with its uncertainty is shown as a straight line. At the crossover point,  $\beta/\alpha$  is 0.30. In Fig. 8, we show the data and DWBA calculations with configuration mixture of  $\beta/\alpha=0.30$ . The normalization factors are 384 and 402 for 0.32- and 5.86-MeV states, respectively. This mixing amplitude implies a two-body mixing matrix element between CK and  $(sd)_{0+}^2$  levels of  $|V|=\alpha\beta\Delta E=1.54$  MeV, quite a reasonable value.

#### IV. CONCLUSION

In the present study of  ${}^9\text{Be}(t,p){}^{11}\text{Be}$  at 15.0 MeV, nine low-lying states were observed, and widths of the four broad states have been measured. Differential cross sections of each state were compared with DWBA calculations. In the calculations, Cohen-Kurath wave functions,  ${}^{10}\text{Be}\otimes(sd)$  configurations, and  ${}^9\text{Be}\otimes(sd)^2$  configurations were used to describe three groups of states. Mixture between different configurations with the same  $L$  transfer is discussed for 0.32- and 5.86-MeV states.

---

\*Present address: University of Notre Dame, Notre Dame, IN 46556.

<sup>1</sup>D. J. Millener, J. W. Olness, E. K. Warburton, and S. S. Hanna, Phys. Rev. C **28**, 497 (1983).

<sup>2</sup>F. Ajzenberg-Selove and C. L. Busch, Nucl. Phys. **A336**, 1 (1980).

<sup>3</sup>A. G. M. van Hees and P. W. M. Glaudemans, Z. Phys. A **315**, 223 (1984).

<sup>4</sup>F. Ajzenberg-Selove, Nucl. Phys. **A433**, 1 (1985).

<sup>5</sup>D. J. Pullen, E. R. Litherland, S. Hinds, and R. Middleton, Nucl. Phys. **36**, 1 (1962).

<sup>6</sup>F. Ajzenberg-Selove, E. R. Flynn, and Ole Hansen, Phys. Rev. C **17**, 1283 (1987).

<sup>7</sup>B. Zwieglinski, W. Benenson, R. G. H. Robertson, and W. R. Coker, Nucl. Phys. **A315**, 124 (1979).

<sup>8</sup>D. L. Auton, Nucl. Phys. **A157**, 305 (1970).

<sup>9</sup>S. Cohen and D. Kurath, Nucl. Phys. **A141**, 145 (1970).

<sup>10</sup>S. Cohen and D. Kurath, Nucl. Phys. **A101**, 1 (1967).

<sup>11</sup>P. D. Kunz, private communication.

<sup>12</sup>S. Mordechai, H. T. Fortune, G. E. Moore, M. E. Cobern, R. V. Kollarits, and R. Middleton, Nucl. Phys. **A301**, 463 (1978).

<sup>13</sup>N. S. E. Darden, G. Murillo, and S. Sen, Nucl. Phys. **A266**, 29 (1976).

<sup>14</sup>R. D. Lawson, F. J. D. Serduke, and H. T. Fortune, Phys. Rev. C **14**, 1245 (1970).